Journal of Zhejiang University-SCIENCE A (Applied Physics & Engineering)
ISSN 1673-565X (Print); ISSN 1862-1775 (Online)
www.jzus.zju.edu.cn; www.springerlink.com
E-mail: jzus@zju.edu.cn

Updated Bayesian detection of foundation parameter with Jeeves pattern search theory*

Jian ZHANG[†1], Chao JIA[†‡2], Chu-wei ZHOU[1]
[1]Department of Mechanics and Structural Engineering, Nanjing University of Aeronautics and Astronautics, Nanjing 210016, China
[2]School of Civil Engineering, Shandong University, Jinan 250061, China
[†]E-mail: zjmech@163.com; jiachao@sdu.edu.cn

Received Oct. 23, 2017; Revision accepted Jan. 15, 2018; Crosschecked Aug. 13, 2018

Abstract: Updated Bayesian detection of foundation parameters in the specific foundation mechanical model was studied based on Jeeves pattern search theory. Firstly, the updated Bayesian objective function for general foundation parameters was derived which could synchronously take the stochastic property of systematic parameters and systematic responses into account. Then the governing differential equations for the Winkler foundation model were gained with elastic Mindlin plate theory and the Fourier close form solution of the foundation model was achieved with the Fourier transform method. After the step length of pattern movement was determined with the quadratic parabolic interpolation method, the updated Bayesian detection of stochastic foundation parameters was resolved with Jeeves pattern search theory and then the corresponding detection procedure was completed. Through particular example analysis, the updated Bayesian detection of stochastic foundation parameters has excellent numerical stability and convergence during iterative processes. Jeeves pattern search theory is unconcerned with the partial derivatives of systematic responses to foundation parameters, and undoubtedly has satisfactory iterative efficiency compared with the available Kalman filtering or conjugate gradient detections of the significant foundation parameters. If the iterative processes are efficiently convergent, it is an important prerequisite that the systematic response assignment should be accurate enough. The derived Jeeves pattern search method with updated Bayesian theory can be applied in other kinds of foundation parameters.

Key words: Jeeves pattern search theory; Updated Bayesian objective function; Detection; Foundation parameters; Fourier close form solution
https://doi.org/10.1631/jzus.A1700573 **CLC number:** TU470

1 Introduction

The parameters of soil used in geotechnical engineering include fuzziness, the inaccuracy of the specific type, and a discrete attribute of quantity. To evaluate the selected soil parameters properly is very important (Carrier III, 2005; Meziane et al., 2014; Zidi et al., 2014; Tan et al., 2016). At present, the commonly used soil medium models include the Winkler foundation model, Pasternac foundation model, Hetenyi foundation model, Reissner foundation model, the semi-infinite elastic foundation model, and the finite depth elastic compression layer model (Silva et al., 2001; Azevedo et al., 2002; Zerwer et al., 2002; Bouderba et al., 2013; Bousahla et al., 2014). Among these foundation models, the Winkler foundation model can accurately simulate the actual working condition of the practical foundation and consequently this model has been widely

‡ Corresponding author
* Project supported by the National Natural Science Foundation of China (No. 11232007), the Natural Science Foundation of Jiangsu Province (No. BK20130787), the Fundamental Research Funds for the Central Universities (No. NS2014003), the Research Fund of Zhejiang Guangchuan Engineering Consulting Co., Ltd. (No. Y1704), the Research Fund of Graduate Education and Teaching Reform of Nanjing University of Aeronautics and Astronautics (NUAA) (No. 2017-2), the Research Fund of Education and Teaching Reform of College of Aerospace Engineering, NUAA (No. 2017-5), China
ORCID: Jian ZHANG, https://orcid.org/0000-0003-2457-9558; Chao JIA, https://orcid.org/0000-0002-2448-894X

used (Al-Hammoud et al., 2011; Xin et al., 2014). In practical engineering, the thickness of plate and concrete strength can be obtained by field test, whereas the foundation parameters can be obtained indirectly by parameter detection methods (Liu and Solecki, 2001; Wen, 2011; Cury et al., 2012). Parameter detection methods have been used in the engineering field. However, they are mainly directed to a static parameter detection model, which means that they cannot synchronously take the effect of changing measuring points and measuring times and the influence of the systematic response into account. It is difficult, therefore, to evaluate and identify parameters comprehensively, and that can affect an exact mechanical analysis of the displacement and stress fields (Nanthakumar et al., 2013, 2016; Hamdia et al., 2016). Although there exist some research results of soil parameter detection with the conjugate gradient method and the Kalman filter method, it is necessary in such cases to calculate the error function of the partial derivatives of the soil parameters, which inevitably causes both low computation efficiency and error accumulation (Zhao, 2007; Zhang et al., 2008). Therefore, the aim of this study is to derive the updated Bayesian detection of foundation parameters with a Jeeves pattern search method. Certainly, the Jeeves pattern search method with updated Bayesian theory has universal significance for different kinds of foundation parameters and only the corresponding foundation model should be considered. In addition, Bayesian theory is widely used because it can consider both the randomness of the systematic parameters and the randomness of the system response. In practical engineering, a systematic response often needs to be tested in different time periods. Unfortunately, in general Bayesian theory, the systematic response at different times is difficult to consider and process simultaneously. It is therefore particularly important to derive a specific Bayesian theory which can take the systematic response at different times simultaneously into account.

Thus, in this study, the most significant work is that the updated Bayesian detection model of stochastic foundation parameters based on Jeeves pattern search theory is derived, in which the efficient updated Bayesian theory of foundation parameters is systematically studied in order to take into account the changeable effect of the measured points, the measured times, and the influence of the systematic response, synchronously. Also, the governing differential equations for a specific foundation are derived and the Fourier close form solution is achieved with the Fourier transform method. Through analysis of typical examples, some key conclusions are summarized in detail.

2 Updated Bayesian objective function of stochastic Winkler parameters

During the process of stochastic detection of the soil medium model with a Jeeves pattern search method, the foundation parameters can be treated as stochastic variables, which are noted as the stochastic vector $\boldsymbol{X}=[x_1\ x_2\ \cdots\ x_m]^{\mathrm{T}}$ (m is the dimension of the vector $\boldsymbol{X}$) to carry the parameter search into execution. From Bayesian theory, it can be noted as

$$f(\boldsymbol{X}\,|\,\boldsymbol{W}^*)=\frac{f(\boldsymbol{W}^*\,|\,\boldsymbol{X})f(\boldsymbol{X})}{f(\boldsymbol{W}^*)},\tag{1}$$

where $f(\boldsymbol{X})$ is the a priori information density function, $f(\boldsymbol{W}^*|\boldsymbol{X})$ is the conditional density function of the systematic response, $f(\boldsymbol{W}^*)$ is the systematic response density function and $f(\boldsymbol{X}|\boldsymbol{W}^*)$ is the posterior information density function. It is presumed that the stochastic foundation parameters $\boldsymbol{X}$ conform to a Gaussian normal distribution, so the a priori information density function $f(\boldsymbol{X})$ can be expressed as

$$\begin{aligned}f(\boldsymbol{X})=&(2\pi)^{-\frac{m}{2}}\left|\boldsymbol{C}_X\right|^{-\frac{1}{2}}\\&\times\exp\left[-\frac{1}{2}(\boldsymbol{X}-\boldsymbol{X}_0)^{\mathrm{T}}\boldsymbol{C}_X^{-1}(\boldsymbol{X}-\boldsymbol{X}_0)\right],\end{aligned}\tag{2}$$

where $\boldsymbol{X}_0$ and $\boldsymbol{C}_X$ are respectively the expectation vector and covariance matrix of the stochastic foundation parameters $\boldsymbol{X}$.

During practical engineering, the systematic responses at the testing nodes must be measured several times and the measured systematic response data $\boldsymbol{W}_i^*$ of each time must be extracted from the total data $\boldsymbol{W}^*$. If the ordinary Bayesian objective function is set up to evaluate parameters, there is much repeated and worthless work. So an updated Bayesian objective function of the stochastic foundation parameters is deduced. The joint density function of $\boldsymbol{W}_i^*$ is $\prod_{i=1}^{n} f(\boldsymbol{W}_i^* \mid \boldsymbol{X})$, where n is the number of measured systematic responses. From the maximum likelihood theory, it can be established as

$$f(\boldsymbol{W}^* \mid \boldsymbol{X}) = (2\pi)^{-\frac{mn}{2}} \prod_{i=1}^{n} \left| \boldsymbol{C}_{\boldsymbol{W}_i^*} \right|^{-\frac{1}{2}} \times \exp\left[-\frac{1}{2} \sum_{i=1}^{n} (\boldsymbol{W}_i^* - \boldsymbol{W}_i)^{\mathrm{T}} \boldsymbol{C}_{\boldsymbol{W}_i^*}^{-1} (\boldsymbol{W}_i^* - \boldsymbol{W}_i) \right], \tag{3}$$

where $\boldsymbol{W}_i = \boldsymbol{W}_i(\boldsymbol{X})$ is the systematic response vector of the computational results. Substituting Eqs. (2) and (3) into Eq. (1), the updated Bayesian objective function J can be derived as

$$J = \sum_{i=1}^{n} (\boldsymbol{W}_i^* - \boldsymbol{W}_i)^{\mathrm{T}} \boldsymbol{C}_{\boldsymbol{W}_i^*}^{-1} (\boldsymbol{W}_i^* - \boldsymbol{W}_i) + (\boldsymbol{X} - \boldsymbol{X}_0)^{\mathrm{T}} \boldsymbol{C}_{\boldsymbol{X}}^{-1} (\boldsymbol{X} - \boldsymbol{X}_0). \tag{4}$$

The updated Bayesian objective function J in Eq. (4) is used in a detection model with Jeeves pattern search theory. In order to attain the variance search result of the stochastic foundation parameters $\boldsymbol{X}$, from Eq. (4) the partial differentiation of updated objective function J to the stochastic foundation parameters $\boldsymbol{X}$ is expressed as

$$\frac{\partial J}{\partial \boldsymbol{X}} = \sum_{i=1}^{n} 2 \left(\frac{\partial \boldsymbol{W}_i}{\partial \boldsymbol{X}} \right)^{\mathrm{T}} \boldsymbol{C}_{\boldsymbol{W}_i^*}^{-1} (\boldsymbol{W}_i - \boldsymbol{W}_i^*) + 2\boldsymbol{C}_{\boldsymbol{X}}^{-1} (\boldsymbol{X} - \boldsymbol{X}_0). \tag{5}$$

When $\boldsymbol{W}_i(\boldsymbol{X})$ is submitted to a Taylor formula expansion at the expectation point $\boldsymbol{X}$ and only the zero and first-order items are reserved, we can obtain:

$$\boldsymbol{W}_i(\boldsymbol{X}) = \boldsymbol{W}_i(\overline{\boldsymbol{X}}) + \boldsymbol{S}_i(\overline{\boldsymbol{X}})(\boldsymbol{X} - \overline{\boldsymbol{X}}), \tag{6}$$

where the sensitivity matrix $\boldsymbol{S}_i(\overline{\boldsymbol{X}}) = \left. \frac{\partial \boldsymbol{W}_i}{\partial \boldsymbol{X}} \right|_{X=\overline{X}}$. Substituting Eq. (6) into Eq. (5), it can be obtained that

$$\frac{\partial J}{\partial \boldsymbol{X}} = \sum_{i=1}^{n} 2\boldsymbol{S}_i^{\mathrm{T}} \boldsymbol{C}_{\boldsymbol{W}_i^*}^{-1} (\overline{\boldsymbol{W}}_i + \boldsymbol{S}_i \boldsymbol{X} - \boldsymbol{S}_i \overline{\boldsymbol{X}} - \boldsymbol{W}_i^*) + 2\boldsymbol{C}_{\boldsymbol{X}}^{-1} (\boldsymbol{X} - \boldsymbol{X}_0), \tag{7}$$

where $\overline{\boldsymbol{W}}_i = \boldsymbol{W}_i(\overline{\boldsymbol{X}})$. When the updated Bayesian objective function J acquires the minimum value, Eq. (7) equals zero and

$$\left[\sum_{i=1}^{n} \boldsymbol{S}_i^{\mathrm{T}} \boldsymbol{C}_{\boldsymbol{W}_i^*}^{-1} \boldsymbol{S}_i + \boldsymbol{C}_{\boldsymbol{X}}^{-1} \right] \boldsymbol{X} = \sum_{i=1}^{n} \boldsymbol{S}_i^{\mathrm{T}} \boldsymbol{C}_{\boldsymbol{W}_i^*}^{-1} (\boldsymbol{W}_i^* - \overline{\boldsymbol{W}}_i + \boldsymbol{S}_i \overline{\boldsymbol{X}}) + \boldsymbol{C}_{\boldsymbol{X}}^{-1} \boldsymbol{X}_0. \tag{8}$$

Postulating $\boldsymbol{H} = \sum_{i=1}^{n} \boldsymbol{S}_i^{\mathrm{T}} \boldsymbol{C}_{\boldsymbol{W}_i^*}^{-1} \boldsymbol{S}_i + \boldsymbol{C}_{\boldsymbol{X}}^{-1}$ and $\boldsymbol{M} = \boldsymbol{H}^{-1} \cdot \left[\boldsymbol{S}_1^{\mathrm{T}} \boldsymbol{C}_{\boldsymbol{W}_1^*}^{-1}, \boldsymbol{S}_2^{\mathrm{T}} \boldsymbol{C}_{\boldsymbol{W}_2^*}^{-1}, \cdots, \boldsymbol{S}_n^{\mathrm{T}} \boldsymbol{C}_{\boldsymbol{W}_n^*}^{-1} \right]$ and from Eq. (8), the achieved value $\hat{\boldsymbol{X}}$ of the foundation parameters $\boldsymbol{X}$ can be written as

$$\hat{\boldsymbol{X}} = (\boldsymbol{I} - \boldsymbol{MS})\boldsymbol{X}_0 + \boldsymbol{MW}^* - \boldsymbol{M}(\overline{\boldsymbol{W}} - \boldsymbol{S}\overline{\boldsymbol{X}}), \tag{9}$$

where $\boldsymbol{I}$ is a unit matrix and $\boldsymbol{W}^* = \left[\boldsymbol{W}_1^*, \boldsymbol{W}_2^*, \cdots, \boldsymbol{W}_n^* \right]^{\mathrm{T}}$, where $\boldsymbol{W}_i^*$ is the vector of measured systematic response data of the ith iteration. $\overline{\boldsymbol{W}} = \left[\overline{\boldsymbol{W}}_1, \overline{\boldsymbol{W}}_2, \cdots, \overline{\boldsymbol{W}}_n \right]^{\mathrm{T}}$, where $\overline{\boldsymbol{W}}_i$ is the systematic response vector of computational data of the ith iteration at the expectation point $\overline{\boldsymbol{X}}$. $\boldsymbol{S} = \left[\boldsymbol{S}_1, \boldsymbol{S}_2, \cdots, \boldsymbol{S}_n \right]^{\mathrm{T}}$, where $\boldsymbol{S}_i$ is the sensitivity matrix of measured systematic responses of the ith iteration. Postulating that the a priori information $\boldsymbol{X}_0$ of the foundation parameters $\boldsymbol{X}$ is irrelevant to the measured systematic response data $\boldsymbol{W}^*$, the variance of $\hat{\boldsymbol{X}}$ in Eq. (9) can be written as

$$\boldsymbol{C}_{\hat{X}} = \left[\boldsymbol{I} - \boldsymbol{MS} \right] \boldsymbol{C}_{\boldsymbol{X}} \left[\boldsymbol{I} - \boldsymbol{MS} \right]^{\mathrm{T}} + \boldsymbol{MC}_{\boldsymbol{W}^*} \boldsymbol{M}^{\mathrm{T}}, \tag{10}$$

where $\boldsymbol{C}_{\boldsymbol{W}^*} = \mathrm{diag}(\boldsymbol{C}_{\boldsymbol{W}_1^*}, \boldsymbol{C}_{\boldsymbol{W}_2^*}, \cdots, \boldsymbol{C}_{\boldsymbol{W}_n^*})$ and $\boldsymbol{C}_{\boldsymbol{W}_i^*}$ is the covariance matrix of measured systematic response data of the ith iteration. Using the non-singularity property of $\boldsymbol{C}_X$ and $\boldsymbol{C}_{\boldsymbol{W}^*}$, Eq. (10) can be transformed into the brief summation form:

$$\boldsymbol{C}_{\hat{X}} = \left[\boldsymbol{C}_X^{-1} + \sum_{i=1}^{n} \boldsymbol{S}_i^{\mathrm{T}} \boldsymbol{C}_{W_i^*}^{-1} \boldsymbol{S}_i \right]^{-1}. \quad (11)$$

3 Theoretic systematic responses for the updated Bayesian objective function

The main suppositions are that the normal line of the middle surface before deformation still remains a straight line after deformation, but it may not be vertical to the middle surface, which means that a transversal shearing deformation effect is admitted and that the stress vertical to the middle surface can be ignored (Bourada et al., 2015; Hamidi et al., 2015; Bennoun et al., 2016). The displacement field of the Mindlin plate in Fig. 1 can be expressed as

$$\begin{cases} u(x,y,z) = z\theta_x(x,y), \\ v(x,y,z) = z\theta_y(x,y), \\ w(x,y,z) = w(x,y), \end{cases} \quad (12)$$

where xy are the rectangular coordinates of the plate plane and z is the thickness coordinate. u, v, and w are respectively the displacements along the x, y, and z directions. θ_x and θ_y are respectively the rotational displacements of the normal lines of the xz plane and yz plane. The equations between updated stress and strain for the Mindlin plate are derived as

$$\boldsymbol{\sigma}_{\mathrm{f}} = \boldsymbol{D}_{\mathrm{f}} \boldsymbol{\varepsilon}_{\mathrm{f}}, \quad (13)$$

$$\boldsymbol{\sigma}_{\mathrm{s}} = \boldsymbol{D}_{\mathrm{s}} \boldsymbol{\varepsilon}_{\mathrm{s}}, \quad (14)$$

where

$$\boldsymbol{\sigma}_{\mathrm{f}} = \left[M_x \;\; M_y \;\; M_{xy} \right]^{\mathrm{T}}, \quad (15)$$

$$\boldsymbol{\sigma}_{\mathrm{s}} = \left[Q_x \;\; Q_y \right]^{\mathrm{T}}, \quad (16)$$

$$\boldsymbol{\varepsilon}_{\mathrm{f}} = \left[\frac{\partial \theta_x}{\partial x} \;\; \frac{\partial \theta_y}{\partial y} \;\; \frac{\partial \theta_x}{\partial y} + \frac{\partial \theta_y}{\partial x} \right]^{\mathrm{T}}, \quad (17)$$

$$\boldsymbol{\varepsilon}_{\mathrm{s}} = \left[\theta_x + \frac{\partial w}{\partial x} \;\; \theta_y + \frac{\partial w}{\partial y} \right]^{\mathrm{T}}, \quad (18)$$

where M_x and M_y are the bending moments respectively along the x and y directions. M_{xy} is the torsion moment. Q_x and Q_y are the shearing forces respectively along the x and y directions. $\boldsymbol{\sigma}_{\mathrm{f}}$ and $\boldsymbol{\varepsilon}_{\mathrm{f}}$ are respectively defined as the updated bending stresses and updated bending strains. $\boldsymbol{\sigma}_{\mathrm{s}}$ and $\boldsymbol{\varepsilon}_{\mathrm{s}}$ are respectively defined as the updated shearing stresses and updated shearing strains. $\boldsymbol{D}_{\mathrm{f}}$ is defined as the bending elastic matrix which is connected with the elastic modulus, Poisson's ratio, and the thickness of the Mindlin plate. $\boldsymbol{D}_{\mathrm{s}}$ is defined as a shearing elastic matrix which is connected with the shearing elastic modulus, the thickness, and the shearing correction coefficient of the Mindlin plate.

When the forces including surface tension are neglected (Belabed et al., 2014; Hebali et al., 2014; Li et al., 2015; Yahia et al., 2015), the governing differential equations for the Mindlin plate on the Winkler foundation can be written as

$$\begin{cases} \dfrac{\partial Q_x}{\partial x} + \dfrac{\partial Q_y}{\partial y} + q - k_z w = 0, \\ \dfrac{\partial M_x}{\partial x} + \dfrac{\partial M_{xy}}{\partial y} - Q_x = 0, \\ \dfrac{\partial M_{xy}}{\partial x} + \dfrac{\partial M_y}{\partial y} - Q_y = 0, \end{cases} \quad (19)$$

where k_z is the Winkler foundation parameter, and q is the load density along the z direction. The boundary conditions of the plate are considered as simply supported. Directly solving the governing differential Eq. (19) is very difficult and therefore the Fourier transform method is used. Substituting Eqs. (13) and (14) into Eq. (19), then the important governing differential Eq. (19) can be turned into differential equations with variables θ_x, θ_y, and w. These variables are then expanded in the form of multiple Fourier series as

$$\begin{cases} \theta_x = \sum\limits_m \sum\limits_n A_{mn} \cos(\xi_m x) \sin(\eta_n y), \\ \theta_y = \sum\limits_m \sum\limits_n B_{mn} \sin(\xi_m x) \cos(\eta_n y), \\ w = \sum\limits_m \sum\limits_n C_{mn} \sin(\xi_m x) \sin(\eta_n y), \end{cases} \quad (20)$$

where m and n are the multiple Fourier series terms. A_{mn}, B_{mn}, and C_{mn} are the undetermined coefficients. ξ_m and η_n are the multiple Fourier expanding coefficients. Based on the multiple Fourier transformation theory, and substituting Eq. (20) into the achieved differential equations with the variables θ_x, θ_y, and w of the Mindlin plate on the Winkler foundation, then the discussed differential equations can be transformed into the linear algebraic equations with the variables A_{mn}, B_{mn}, and C_{mn}, which can be easily solved. After the undetermined coefficients A_{mn}, B_{mn}, and C_{mn} are settled and then substituted back into Eq. (20), the displacement field functions θ_x, θ_y, and w of the Mindlin plate are obtained, which are viewed as the necessary theoretical systematic responses during updated Bayesian detection of the Winkler foundation parameters with the Jeeves pattern search method.

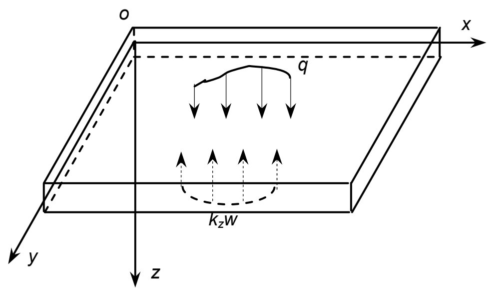

Fig. 1 Mindlin plate on Winkler foundation

4 Detection of the stochastic foundation parameters with the Jeeves pattern search theory

4.1 Jeeves pattern search theory

The available optimization methods are of two main types: the first is a direct search method such as the Jeeves pattern search method or revised Powell method, and the second is a gradient search method such as the Broden-Fletcher-Goldfarb-Shanno (BFGS) method or conjugate gradient method. The gradient search method continuously changes the matrix scale to produce new searching directions during the optimization iterative processes. The gradient optimization method has to determine the partial differentiations of objective functions to systematic parameters, which inevitably leads to error accumulation. The same is true for the Kalman filtering method. Among the direct search methods, the Jeeves pattern search method, which is formed and improved from the variable alternate method, tries to optimize the updated Bayesian objective function along each coordinate orientation. This is defined as a detective search. After the detective search, the variational regularity of the studied objective function is achieved and consequently the optimal search direction is determined. Then, the studied objective function is moved along the special direction and evaluated at the optimal spatial point. This is defined as pattern movement. The main two stages are alternated until the detective step length is less than the given criterion.

Combined with updated Bayesian theory, the flowchart for detection of the foundation parameters with the Jeeves pattern search method is shown in Fig. 2 and the corresponding steps are presented as follows:

1. Select the initial foundation parameter vector $\boldsymbol{X}^0$ and the initial step length vector $\boldsymbol{t}^0$. The step length t_i^0 along the ith coordinate direction in $\boldsymbol{t}^0$ can usually be determined as

$$t_i^0 = \lambda(\overline{x}_i - \underline{x}_i), \quad i = 1, 2, \cdots, n, \tag{21}$$

where $\overline{x}_i$ and $\underline{x}_i$ are respectively the possible upper and lower bounds of x_i which can roughly be assigned from engineering experience. λ may be assumed as 0.1. n is the dimension of the vector $\boldsymbol{X}^0$.

2. Select the convergence tolerance ε. Define k as the iterative time and let k=0.

3. Let $\boldsymbol{X}^{k,0}=\boldsymbol{X}^k$. Then denote $\boldsymbol{e}_i$ as the ith unit coordinate direction vector and $\boldsymbol{X}^{k,i}$ as the detective point along the direction $\boldsymbol{e}_i$ in the kth iterative time. $\boldsymbol{X}^{k,i}$ is completed by the equations:

$$\begin{aligned} &\boldsymbol{X}^{k,i} = \boldsymbol{X}^{k,i-1} + t_i^k \boldsymbol{e}_i, \\ &J(\boldsymbol{X}^{k,i-1} + t_i^k \boldsymbol{e}_i) < J(\boldsymbol{X}^{k,i-1}), \end{aligned} \tag{22}$$

$$\begin{aligned} &\boldsymbol{X}^{k,i} = \boldsymbol{X}^{k,i-1} - t_i^k \boldsymbol{e}_i, \\ &J(\boldsymbol{X}^{k,i-1} - t_i^k \boldsymbol{e}_i) < J(\boldsymbol{X}^{k,i-1}) \le J(\boldsymbol{X}^{k,i-1} + t_i^k \boldsymbol{e}_i), \end{aligned} \tag{23}$$

$$\begin{aligned} &\boldsymbol{X}^{k,i} = \boldsymbol{X}^{k,i-1}, \\ &J(\boldsymbol{X}^{k,i-1} - t_i^k \boldsymbol{e}_i) \ge J(\boldsymbol{X}^{k,i-1}) < J(\boldsymbol{X}^{k,i-1} + t_i^k \boldsymbol{e}_i), \end{aligned} \tag{24}$$

where i=1, 2, …, n.

4. If the detective search stage is finished, which means i=n, and $\boldsymbol{X}^{k,n}\neq\boldsymbol{X}^{k,0}$, it turns into the pattern movement stage of step 7.

5. If $\boldsymbol{X}^{k,n}=\boldsymbol{X}^{k,0}$, it is clarified that the optimal search direction cannot be obtained from $\boldsymbol{X}^k$ with the available step length and so the step length must be decreased.

6. Let $\boldsymbol{t}^k=\beta\boldsymbol{t}^k$, where β is the reduction coefficient which may be assumed as 0.5. If the condition $\max_i |t_i^k| \le \varepsilon$ is satisfied, $\boldsymbol{X}^k$ is the convergence solution. The iteration is terminated and we go to step 11. Otherwise go back to step 3.

7. The vector $\boldsymbol{X}^{k,n}-\boldsymbol{X}^k$ is considered as the progressive movement direction. Then the point $\tilde{\boldsymbol{X}}^k$ can be ascertained as

$$\tilde{\boldsymbol{X}}^k = \boldsymbol{X}^{k,n} + \alpha^k(\boldsymbol{X}^{k,n} - \boldsymbol{X}^k), \qquad (25)$$

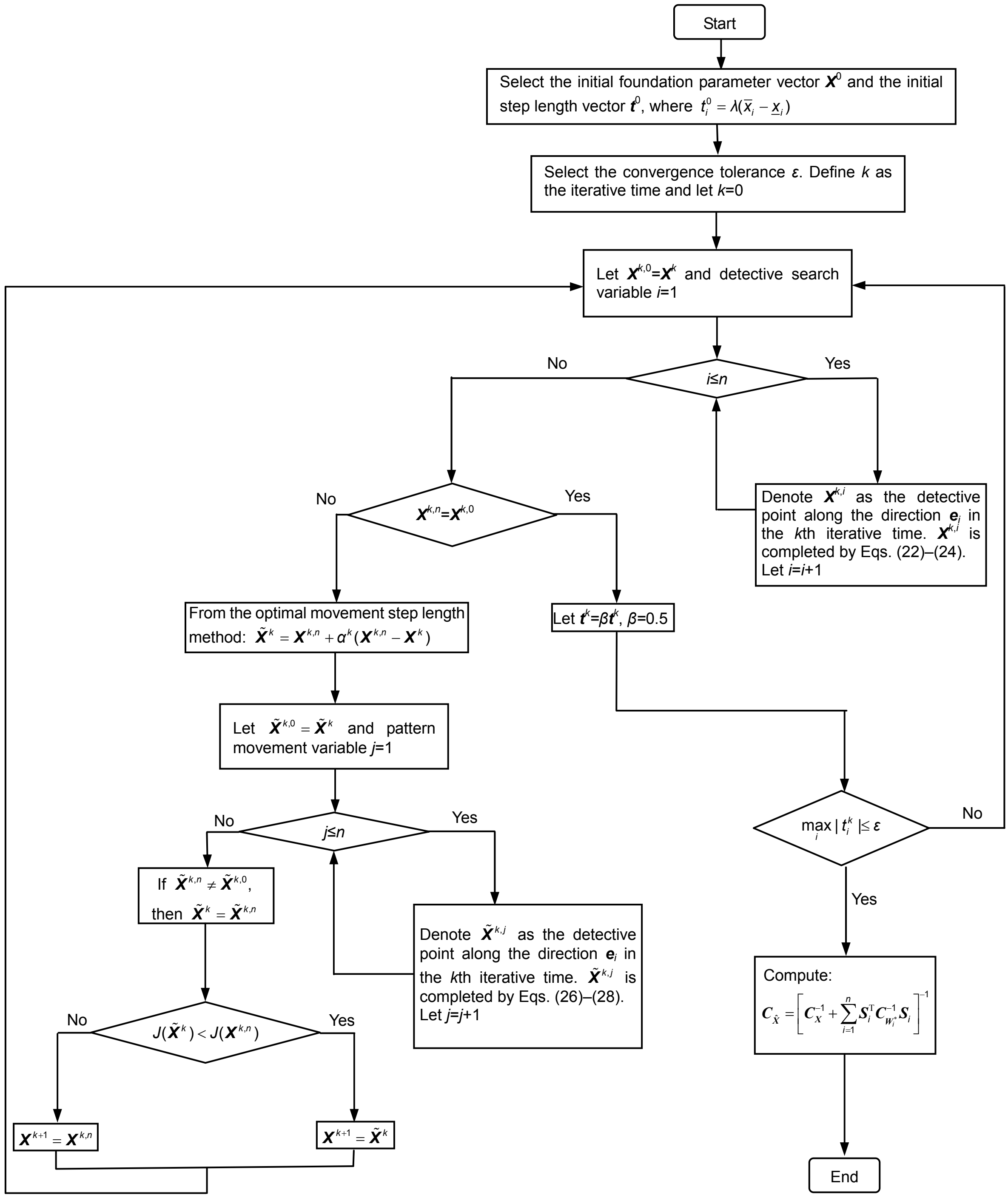

Fig. 2 Flowchart for updated Bayesian detection of the foundation parameters with a Jeeves pattern search method

where α^k is the optimal movement step length, which is determined by a 1D search method such as the Fibonacci interpolation method or the quadratic parabolic interpolation method.

8. Let $\tilde{\boldsymbol{X}}^{k,0}=\tilde{\boldsymbol{X}}^{k}$. From $\tilde{\boldsymbol{X}}^{k}$, then $\tilde{\boldsymbol{X}}^{k,j}$ is completed by the following equations:

$$\tilde{\boldsymbol{X}}^{k,j}=\tilde{\boldsymbol{X}}^{k,j-1}+t_j^k\boldsymbol{e}_j,\quad J(\tilde{\boldsymbol{X}}^{k,j-1}+t_j^k\boldsymbol{e}_j)<J(\tilde{\boldsymbol{X}}^{k,j-1}),\tag{26}$$

$$\tilde{\boldsymbol{X}}^{k,j}=\tilde{\boldsymbol{X}}^{k,j-1}-t_j^k\boldsymbol{e}_j,\quad J(\tilde{\boldsymbol{X}}^{k,j-1}-t_j^k\boldsymbol{e}_j)<J(\tilde{\boldsymbol{X}}^{k,j-1})\le J(\tilde{\boldsymbol{X}}^{k,j-1}+t_j^k\boldsymbol{e}_j),\tag{27}$$

$$\tilde{\boldsymbol{X}}^{k,j}=\tilde{\boldsymbol{X}}^{k,j-1},\quad J(\tilde{\boldsymbol{X}}^{k,j-1}-t_j^k\boldsymbol{e}_j)\ge J(\tilde{\boldsymbol{X}}^{k,j-1})<J(\tilde{\boldsymbol{X}}^{k,j-1}+t_j^k\boldsymbol{e}_j),\tag{28}$$

where j=1, 2, …, n.

9. If j=n and $\tilde{\boldsymbol{X}}^{k,n}\ne\tilde{\boldsymbol{X}}^{k,0}$, then $\tilde{\boldsymbol{X}}^{k}=\tilde{\boldsymbol{X}}^{k,n}$. Otherwise, $\tilde{\boldsymbol{X}}^{k}$ is kept unchanged.

10. If $J(\tilde{\boldsymbol{X}}^{k})<J(\boldsymbol{X}^{k,n})$, it means that the pattern movement is successful and $\boldsymbol{X}^{k+1}=\tilde{\boldsymbol{X}}^{k}$. If $J(\tilde{\boldsymbol{X}}^{k})\ge J(\boldsymbol{X}^{k,n})$, it means that the pattern movement fails and $\boldsymbol{X}^{k+1}$=$\boldsymbol{X}^{k,n}$. Then we go back to step 3 of detective search and begin a new turn of iteration.

11. From Eq. (11), the covariance $\boldsymbol{C}_{\hat{X}}$ of the Winkler foundation parameters $\boldsymbol{X}$ is achieved.

4.2 Determination of the optimal step length

Searching the optimal step length is necessary in step 7 of the updated Bayesian detection steps of the foundation parameters, which is a fairly complicated problem in the analysis of parameter detection (Zhang et al., 2010; Vu-Bac et al., 2016; Hamdia et al., 2017). Of the available achievements, the 1D search method is generally preferred to the golden section method or quadratic parabolic interpolation method. Among these methods, the quadratic parabolic interpolation method has greater computational efficiency, which can automatically determine the span of the optimal movement step length α and then optimize the significant step length. The main steps include:

1. Determination of the span where the optimal step length α lies. Assume the initial step length α_1 and a step length increment α_0 and set α_2=α_1+α_0. From the updated Bayesian objective function, if $J(\alpha_1)\ge J(\alpha_2)$, the step length increment defined as α_k=α_{k-1}+$2^{k-2}\alpha_0$, where $k\ge3$, is calculated. The calculation is not ended until $J(\alpha_k)\ge J(\alpha_{k-1})$. If $J(\alpha_1)<J(\alpha_2)$, the other step length increment is defined as α_k=α_{k-1}+$2^{k-3}\alpha_0$, where $k\ge3$, and calculated. Similarly, the calculation is not ended until $J(\alpha_k)\ge J(\alpha_{k-1})$. When the iterative calculation is completed, the interval of the optimal step length α is obtained and noted as [α_a, α_d], where α_a and α_d are the values of the two endpoints of the interval where the optimal movement step length α lies.

2. Interpolation of the optimal step length α. On the basis of the function extremum theory of the Bayesian objective function and through pertinent mathematical deductions, the optimal step length α is presented:

$$\alpha=\frac{1}{2}\left(\alpha_a+\alpha_d-\frac{\alpha_b}{\alpha_c}\right),\tag{29}$$

$$\alpha_b=\frac{J(\alpha_d)-J(\alpha_a)}{\alpha_d-\alpha_a},\tag{30}$$

$$\alpha_c=\frac{1}{\alpha_e-\alpha_d}\left[\frac{J(\alpha_e)-J(\alpha_a)}{\alpha_e-\alpha_a}-\alpha_b\right],\tag{31}$$

where α_b and α_c are both the transitional variables. α_e is the middle point of the interval [α_a, α_d].

5 Example analysis of the updated Bayesian detection of the stochastic foundation parameters

5.1 Analytical material

In order to take the updated Bayesian detection of the stochastic foundation parameters with Jeeves pattern search theory into action, the detection program named JEVFND.for is compiled in which the subprogram of a Fourier close form solution is employed. Three different kinds of Winkler foundations in Fig. 3, on which three different concrete bearing plates are respectively settled, are taken into account. The dimension, elastic modulus, Poisson's ratio, and the shearing correction coefficient of the plates and both the true value and the coefficient of variation of the Winkler foundations are presented in Table 1. The uniform loads q_1 and q_2, which are respectively equal to 300.0 N/cm^2 and 180.0 N/cm^2 along the z

coordinate direction, are respectively applied on the concrete bearing plate on the first and second Winkler foundations, and the concentrated load P which equals 2500 kN is applied on the concrete bearing plate on the third Winkler foundation. The four selected points on the concrete bearing plate in Fig. 4 are viewed as displacement-measured spots and the displacement of each selected point is measured five times with consideration of the measured error. The measured displacement data and the displacement standard deviation data are listed in Table 2 (Sun et al., 1996) and the numerical changes represent the randomness of the system response.

5.2 Convergence verification of Jeeves pattern search model

In order to validate the reliability of the Jeeves pattern search model of the stochastic foundation parameter and the correctness of the completed analytical program, the a priori information of the stochastic foundation parameter is firstly presupposed to satisfy the precise condition. The a priori information data of the three Winkler foundation parameters are

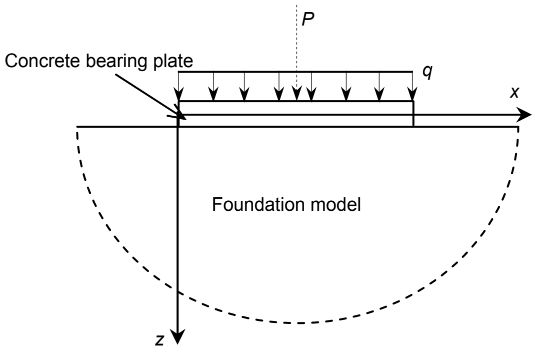

Fig. 3 Concrete bearing plate on a Winkler foundation

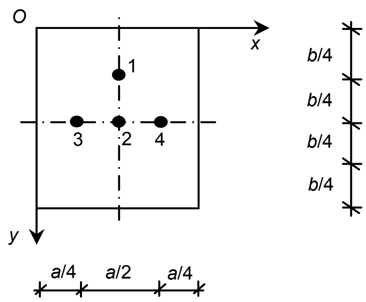

Fig. 4 Four selected points on the concrete bearing plate

Table 1 Dimensions of the concrete bearing plate and other parameters

Foundation No.	Plate length, a (cm)	Plate width, b (cm)	Plate thickness, t (cm)	Elastic modulus, E (N/cm^2)	Poisson's ratio, μ	Shearing correction coefficient, γ	Winkler parameter, k_z (N/cm^3)	Coefficient of variation, η
1	120	160	10	3.0×10^6	0.16	0.8	110	0.1
2	100	80	8	3.2×10^6	0.16	0.8	80	0.1
3	60	120	10	3.0×10^6	0.16	0.8	60	0.1

Table 2 Displacement measurement and the displacement standard deviation

Foundation No.	Selected points No.	Displacement measurement (cm)					Displacement standard deviation (cm)				
		w_1	w_2	w_3	w_4	w_5	σ_{w1}	σ_{w2}	σ_{w3}	σ_{w4}	σ_{w5}
1	1	0.877	0.873	0.879	0.871	0.872	0.013	0.016	0.015	0.011	0.018
	2	1.175	1.171	1.179	1.173	1.172	0.025	0.023	0.028	0.022	0.027
	3	0.849	0.843	0.846	0.842	0.845	0.012	0.016	0.018	0.010	0.015
	4	0.850	0.853	0.848	0.855	0.856	0.015	0.018	0.012	0.016	0.019
2	1	0.216	0.213	0.215	0.212	0.219	0.007	0.011	0.012	0.009	0.008
	2	0.299	0.293	0.292	0.297	0.294	0.011	0.008	0.009	0.006	0.012
	3	0.220	0.224	0.223	0.227	0.217	0.012	0.005	0.007	0.010	0.009
	4	0.218	0.223	0.214	0.215	0.213	0.010	0.006	0.008	0.004	0.007
3	1	0.281	0.283	0.284	0.278	0.277	0.011	0.008	0.009	0.008	0.010
	2	0.728	0.723	0.725	0.732	0.731	0.041	0.045	0.036	0.039	0.043
	3	0.397	0.393	0.395	0.403	0.402	0.006	0.010	0.009	0.008	0.011
	4	0.401	0.404	0.398	0.397	0.403	0.013	0.006	0.007	0.011	0.008

respectively 110 N/cm^3, 80 N/cm^3, and 60 N/cm^3. The two groups of the initial parameter data k_{10} and k_{20} are set as 180 N/cm^3 and 25 N/cm^3, respectively. The convergence tolerances of ε are equal to 0.001. With the displacement measurement and the displacement standard deviation shown in Table 2, the Jeeves pattern search results are achieved in Fig. 5 and Table 3.

It is shown in Fig. 5 and Table 3 that although different initial foundation parameter data are set, the relative errors of the foundation parameters are far less than 5% and the Jeeves pattern iterative processes are steadily convergent to the true values, indicating that the updated Bayesian detection of the foundation parameter is correct and the completed program is reliable. The coefficient of variation is about 0.074, which is improved with the given data. From the search mechanical model analysis, unlike the Kalman filtering theory and the conjugate gradient theory, the partial derivatives of the systematic responses to the foundation parameters are not involved in the iterative detection processes, which consequentially leads to higher computational efficiency.

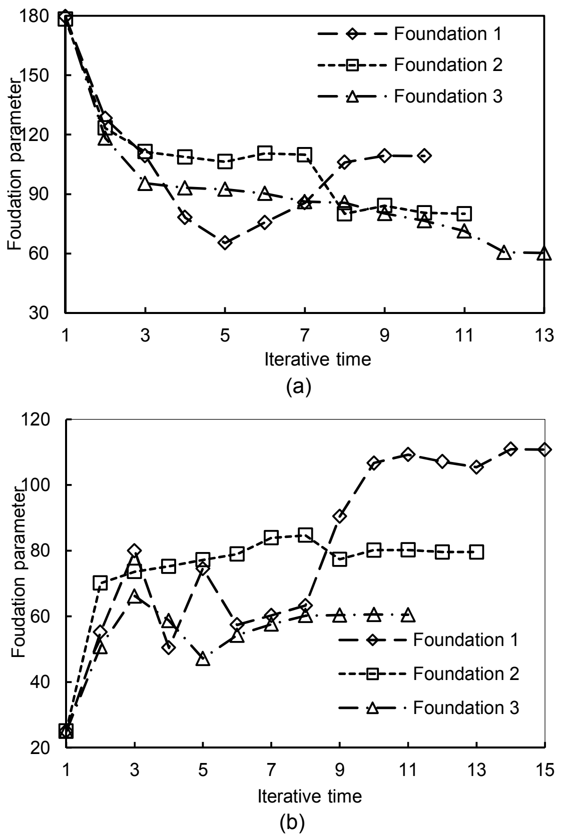

Fig. 5 Jeeves pattern iterative process in convergence verification: (a) k_{10}; (b) k_{20}

The updated Bayesian theoretical model for the Winkler foundation parameters has universal significance for different kinds of foundation parameters and only the corresponding foundation model should be considered and substituted (Beldjelili et al., 2016; Bounouara et al., 2016; Besseghier et al., 2017; Zhang et al., 2017). Besides, the Jeeves pattern search method can be replaced by some other optimization methods and the corresponding analytical models will be achieved naturally.

5.3 Stability verification of the Jeeves pattern search model

The a priori information of the foundation parameter is supposed not to satisfy the precise condition, which means that the deviation degree of the a priori information from the true parameter value exceeds 10%. From large quantities of trial computations, the Jeeves pattern iterative processes are always divergent because the two items in Eq. (4) cannot simultaneously converge in accordance with the set criteria. In practical engineering, the a priori information cannot be always precisely grasped and in this section, the second item in Eq. (4) should be deleted and the discussed updated Bayesian objective function should be evolved into the extensive Markov form (Wen, 2011). The initial parameter data k_{10} and k_{20} are set as 180 N/cm^3 and 30 N/cm^3, respectively. The rest of the data are the same as Section 5.2, and from the developed program, the Jeeves pattern detection results are found from Fig. 6 and Table 4.

Table 3 Jeeves pattern search results in convergence verification

Foundation No.	k_{10}				k_{20}			
	Final parameter (N/cm^3)	Iterative time	Relative error (%)	Convergent	Final parameter (N/cm^3)	Iterative time	Relative error (%)	Convergent
1	109.213	10	0.715	Yes	110.733	15	0.666	Yes
2	80.015	11	0.012	Yes	79.558	13	0.552	Yes
3	60.231	13	0.385	Yes	60.436	11	0.723	Yes

From the results in Fig. 6 and Table 4, the Jeeves pattern iterative processes are also steadily convergent to the true values. Compared with the results for the Bayesian objective function in Section 5.2, the relative errors of the foundation parameters are also far less than 5%. It is illustrated again, therefore, that the Jeeves pattern search model of the foundation parameter is a convincing one (Sun et al., 1996; Zhang et al., 2010). In this section, it is an improvement that the partial derivatives of the systematic responses to the Winkler foundation parameters are not needed for the Jeeves pattern iterative process. From the results, it is shown that when the different initial parameter values are assumed, they are all convergent to the true values, and the convergence is relatively insensitive to the selection of the initial parameter values.

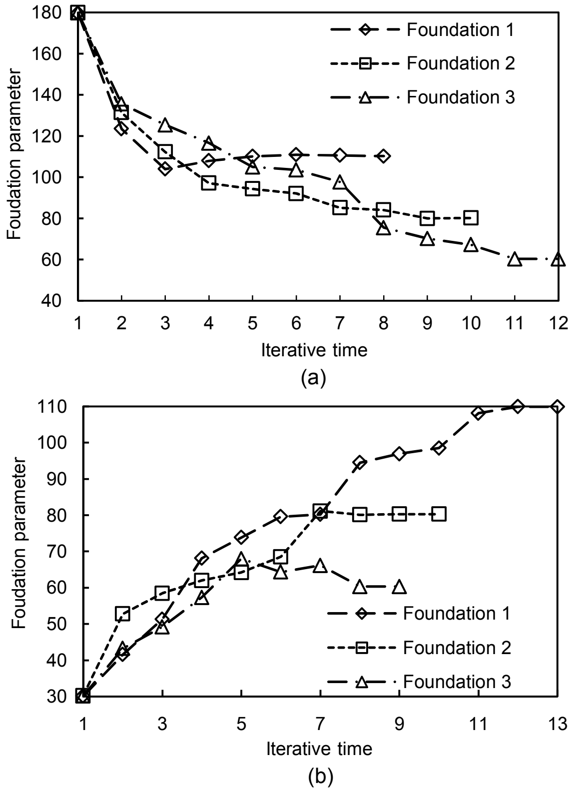

Fig. 6 Jeeves pattern iterative process in stability verification: (a) k_{10}; (b) k_{20}

5.4 Sensitivity analysis of measured response in the Jeeves pattern search model

The measured displacement data are not precise, which means the deviation degree of the measured data from the true data in Table 2 is set as 15%. The a priori information of the Winkler foundation parameter is presumed to conform to the precise condition and the other data are similar with those in Section 5.2. From the developed program, the Jeeves pattern search results are listed in Table 5.

It is indicated from the results in Table 5 that when the measured displacement data are imprecise, the Jeeves pattern iterative processes of the Winkler foundation parameter are divergent and the relative errors are far more than 5% even though the iterations reach a fairly large number. The computational results prove that the precision of the measured systematic response is of great importance, which means the systematic responses must be accurately supplied, otherwise the Jeeves pattern iterative process cannot

Table 4 Jeeves pattern search results in stability verification

Foundation No.	k_{10}				k_{20}			
	Final parameter (N/cm^3)	Iterative time	Relative error (%)	Convergent	Final parameter (N/cm^3)	Iterative time	Relative error (%)	Convergent
1	110.247	8	0.224	Yes	109.876	13	0.113	Yes
2	80.276	10	0.345	Yes	80.314	10	0.393	Yes
3	60.325	12	0.542	Yes	60.317	9	0.528	Yes

Table 5 Jeeves pattern search results in sensitivity analysis of measured response

Foundation No.	k_{10}				k_{20}			
	Final parameter (N/cm^3)	Iterative time	Relative error (%)	Convergent	Final parameter (N/cm^3)	Iterative time	Relative error (%)	Convergent
1	147.482	100	34.075	No	84.715	100	22.986	No
2	98.803	100	17.094	No	62.573	100	15.843	No
3	77.815	100	29.692	No	44.547	100	25.755	No

be efficiently completed. It can be seen that the convergence is relatively sensitive to the assignment of the measured displacement data, and if the Jeeves pattern iterative processes are efficiently convergent, it is an important prerequisite that the systematic response assignment should be accurate enough.

6 Conclusions

1. An updated Bayesian detection model of the stochastic Winkler foundation parameter based on Jeeves pattern search theory is derived. The Jeeves pattern iterative processes are steadily convergent to the true values, indicating that the derived detection model is correct and reliable.

2. Unlike the Kalman filtering theory and the conjugate gradient theory, the partial derivatives of the systematic responses to the foundation parameters are irrelevant in the Jeeves pattern search process, which indicates that the Jeeves pattern theory is of higher computational efficiency.

3. Searching for the optimal movement step length is a fairly complicated problem in parameter detection. The derived quadratic parabolic interpolation method can automatically determine the interval of the optimal step length and then search the significant step length.

4. The derived updated Bayesian detection model based on the Jeeves pattern search theory has universal significance for different kinds of foundation parameters if the corresponding foundation model is considered and substituted for the discussed Winkler foundation.

References

Al-Hammoud R, Soudki K, Topper TH, 2011. Fatigue flexural behavior of corroded reinforced concrete beams repaired with CFRP sheets. *Journal of Composites for Construction*, 15(1):42-51. https://doi.org/10.1061/(asce)cc.1943-5614.0000144

Azevedo RF, Parreira AB, Zornberg JG, 2002. Numerical analysis of a tunnel in residual soils. *Journal of Geotechnical and Geoenvironmental Engineering*, 128(3): 227-236. https://doi.org/10.1061/(asce)1090-0241(2002)128:3(227)

Belabed Z, Houari MSA, Tounsi A, et al., 2014. An efficient and simple higher order shear and normal deformation theory for functionally graded material (FGM) plates. *Composites Part B*: *Engineering*, 60:274-283. https://doi.org/10.1016/j.compositesb.2013.12.057

Beldjelili Y, Tounsi A, Mahmoud SR, 2016. Hygro-thermo-mechanical bending of S-FGM plates resting on variable elastic foundations using a four-variable trigonometric plate theory. *Smart Structures and Systems*, 18(4):755-786. https://doi.org/10.12989/sss.2016.18.4.755

Bennoun M, Houari MSA, Tounsi A, 2016. A novel five-variable refined plate theory for vibration analysis of functionally graded sandwich plates. *Mechanics of Advanced Materials and Structures*, 23(4):423-431. https://doi.org/10.1080/15376494.2014.984088

Besseghier A, Houari MSA, Tounsi A, et al., 2017. Free vibration analysis of embedded nanosize FG plates using a new nonlocal trigonometric shear deformation theory. *Smart Structures and Systems*, 19(6):601-614. https://doi.org/10.12989/sss.2017.19.6.601

Bouderba B, Houari MSA, Tounsi A, 2013. Thermomechanical bending response of FGM thick plates resting on Winkler-Pasternak elastic foundations. *Steel and Composite Structures*, 14(1):85-104. https://doi.org/10.12989/scs.2013.14.1.085

Bounouara F, Benrahou KH, Belkorissat I, et al., 2016. A nonlocal zeroth-order shear deformation theory for free vibration of functionally graded nanoscale plates resting on elastic foundation. *Steel and Composite Structures*, 20(2):227-249. https://doi.org/10.12989/scs.2016.20.2.227

Bourada M, Kaci A, Houari MSA, et al., 2015. A new simple shear and normal deformations theory for functionally graded beams. *Steel and Composite Structures*, 18(2): 409-423. https://doi.org/10.12989/scs.2015.18.2.409

Bousahla AA, Houari MSA, Tounsi A, et al., 2014. A novel higher order shear and normal deformation theory based on neutral surface position for bending analysis of advanced composite plates. *International Journal of Computational Methods*, 11(6):1350082. https://doi.org/10.1142/S0219876213500825

Carrier III WD, 2005. Pipeline supported on a nonuniform Winkler soil model. *Journal of Geotechnical and Geoenvironmental Engineering*, 131(10):1301-1304. https://doi.org/10.1061/(asce)1090-0241(2005)131:10(1301)

Cury A, Cremona C, Dumoulin J, 2012. Long-term monitoring of a PSC box girder bridge: operational modal analysis, data normalization and structural modification assessment. *Mechanical Systems and Signal Processing*, 33:13-37. https://doi.org/10.1016/j.ymssp.2012.07.005

Hamdia KM, Zhuang XY, He PF, et al., 2016. Fracture toughness of polymeric particle nanocomposites: evaluation of models performance using Bayesian method. *Composites Science and Technology*, 126:122-129. https://doi.org/10.1016/j.compscitech.2016.02.012

Hamdia KM, Silani M, Zhuang XY, et al., 2017. Stochastic analysis of the fracture toughness of polymeric nanoparticle composites using polynomial chaos expansions. *International Journal of Fracture*, 206(2):215-227. https://doi.org/10.1007/s10704-017-0210-6

Hamidi A, Houari MSA, Mahmoud SR, et al., 2015. A sinusoidal plate theory with 5-unknowns and stretching effect for thermomechanical bending of functionally graded sandwich plates. *Steel and Composite Structures*, 18(1): 235-253. https://doi.org/10.12989/scs.2015.18.1.235

Hebali H, Tounsi A, Houari MSA, et al., 2014. New quasi-3D hyperbolic shear deformation theory for the static and free vibration analysis of functionally graded plates. *Journal of Engineering Mechanics*, 140(2):374-383. https://doi.org/10.1061/(asce)em.1943-7889.0000665

Li TC, Lyu LX, Zhang SL, et al., 2015. Development and application of a statistical constitutive model of damaged rock affected by the load-bearing capacity of damaged elements. *Journal of Zhejiang University-SCIENCE A (Applied Physics & Engineering)*, 16(8):644-655. https://doi.org/10.1631/jzus.A1500034

Liu XB, Solecki R, 2001. Green's function for an infinite elastic plate on Winkler's foundation. *Journal of Engineering Mechanics*, 127(3):305-307. https://doi.org/10.1061/(asce)0733-9399(2001)127:3(305)

Meziane MAA, Abdelaziz HH, Tounsi A, 2014. An efficient and simple refined theory for buckling and free vibration of exponentially graded sandwich plates under various boundary conditions. *Journal of Sandwich Structures & Materials*, 16(3):293-318. https://doi.org/10.1177/1099636214526852

Nanthakumar SS, Lahmer T, Rabczuk T, 2013. Detection of flaws in piezoelectric structures using extended FEM. *International Journal of Numerical Methods in Engineering*, 96(6):373-389. https://doi.org/10.1002/nme.4565

Nanthakumar SS, Lahmer T, Zhuang X, et al., 2016. Detection of material interfaces using a regularized level set method in piezoelectric structures. *Inverse Problems in Science and Engineering*, 24(1):153-176. https://doi.org/10.1080/17415977.2015.1017485

Silva MA, Swan CC, Arora JS, et al., 2001. Failure criterion for RC members under biaxial bending and axial load. *Journal of Structural Engineering*, 127(8):922-929. https://doi.org/10.1061/(asce)0733-9445(2001)127:8(922)

Sun J, Jiang SP, Yuan Y, et al., 1996. Stochastic Back Analysis Theory and Method of Geotechnical Mechanics. Shantou University Press, Shantou, China, p.68-90 (in Chinese).

Tan P, Ma JE, Zhou J, et al., 2016. Sustainability development strategy of China's high speed rail. *Journal of Zhejiang University-SCIENCE A (Applied Physics & Engineering)*, 17(12): 923-932. http://dx.doi.org/10.1631/jzus.A1600747

Vu-Bac N, Lahmer T, Zhuang X, et al., 2016. A software framework for probabilistic sensitivity analysis for computationally expensive models. *Advances in Engineering Software*, 100:19-31. https://doi.org/10.1016/j.advengsoft.2016.06.005

Wen QJ, 2011. Long-term effect analysis of prestressed concrete box-girder bridge widening. *Construction and Building Materials*, 25(4):1580-1586. https://doi.org/10.1016/j.conbuildmat.2010.09.041

Xin Y, Zhang J, Han XD, et al., 2014. Research on ultimate load of highway prestressed concrete U-shaped continuous rigid frame bridge based on nonlinear finite method. *Applied Mechanics and Materials*, 501-504:1398-1402. https://doi.org/10.4028/www.scientific.net/amm.501-504.1398

Yahia SA, Atmane HA, Houari MSA, et al., 2015. Wave propagation in functionally graded plates with porosities using various higher-order shear deformation plate theories. *Structural Engineering and Mechanics*, 53(6):1143-1165. https://doi.org/10.12989/sem.2015.53.6.1143

Zerwer A, Cascante G, Hutchinson J, 2002. Parameter estimation in finite element simulations of Rayleigh waves. *Journal of Geotechnical and Geoenvironmental Engineering*, 128(3):250-261. https://doi.org/10.1061/(asce)1090-0241(2002)128:3(250)

Zhang J, Ye JS, Tang XS, 2008. Kalman filtering identification of Winkler foundation's parameter based on Mindlin theory. *Rock and Soil Mechanics*, 29(2):425-430 (in Chinese). https://doi.org/10.3969/j.issn.1000-7598.2008.02.025

Zhang J, Zhou CW, Lan WG, et al., 2010. Nonlinear dynamical identification of displacement parameters of multi-cell curve box based on Markov error theory. *Chinese Journal of Applied Mechanics*, 27(4):746-750 (in Chinese).

Zhang J, Zhou CW, Jia C, et al., 2017. Powell inversion mechanical model of foundation parameters with generalized Bayesian theory. *Journal of Zhejiang University-SCIENCE A (Applied Physics & Engineering)*, 18(7): 567-578. https://doi.org/10.1631/jzus.A1600440

Zhao XM, 2007. Dynamic Bayesian identification of Winkler subgrade parameter based on Mindlin theory. *Engineering Mechanics*, 24(10):57-63 (in Chinese). https://doi.org/10.3969/j.issn.1000-4750.2007.10.011

Zidi M, Tounsi A, Houari MSA, et al., 2014. Bending analysis of FGM plates under hygro-thermo-mechanical loading using a four variable refined plate theory. *Aerospace Science and Technology*, 34:24-34. https://doi.org/10.1016/j.ast.2014.02.001

中文概要

题　目：基于 **Jeeves** 模式搜索理论地基参数的更新 **Bayes** 探测法

目　的：通过 Jeeves 模式搜索理论建立弹性地基参数的更新 Bayes 探测分析模型，以及获得地基参数的寻优搜索结果。

创新点： 1. 根据 Bayes 统计理论，推导更新 Bayes 误差函数。2. 结合最优步长的抛物线插值理论，推求地基参数的 Jeeves 模式搜索寻优方法，建立地基参数的探测分析模型。

方　法： 1. 根据 Bayes 统计理论，推导更新 Bayes 误差函数（公式（4））及误差函数对地基参数的梯度表达式（公式（5））。2. 根据中厚度弹性地基板理论，推求 Winkler 地基上板的控制微分方程（公式（19））和 Fourier 闭式解（公式（20））。3. 提出最优步长的抛物线插值寻优方案，并结合 Jeeves 模式搜索理论建立弹性地基参数的更新 Bayes 探测分析模型。

结　论： 1. 基于更新 Bayes 理论，可研究地基参数的 Jeeves 模式搜索分析模型，且地基参数的探测迭代过程具有良好的稳定性与收敛性。2. 更新 Bayes 误差函数能同时考虑不同量测次数和不同测点的位移实测信息，计算效率较高。3. 与共轭梯度法和 Kalman 滤波方法不同的是，Jeeves 模式搜索理论的迭代过程不涉及误差函数偏导数计算，避免了迭代过程的误差累积。

关键词： Jeeves 模式搜索理论；更新 Bayes 误差函数；探测；地基参数；Fourier 闭式解